Variation of the Interfacial Shear Strength and Adhesion of a Nanometer-Sized Contact

R. W. Carpick,† N. Agraït,‡ D. F. Ogletree, and M. Salmeron*

Materials Sciences Division, Lawrence Berkeley National Laboratory, Berkeley, California 94720

Received October 17, 1995. In Final Form: April 10, 1996⊗

We observe that the frictional force between a platinum-coated atomic force microscope (AFM) tip and the surface of mica in ultrahigh vacuum (UHV) varies with load in proportion to the contact area predicted by the Johnson−Kendall−Roberts (JKR) theory (*Proc. R. Soc. London, Ser. A* **1971**, *324*, 301) of adhesive elastic contacts. Using the JKR theory, the interfacial adhesion energy and shear strength can be determined. During the experiment, the tip−sample adhesion unexpectedly decreased by more than one order of magnitude, as did the measured frictional forces . These changes were induced by scanning the tip in contact with the mica sample. We attribute the substantial friction and adhesion decreases to changes of the interface, either structural or chemical, as opposed to changes in bulk structure or properties. The interfacial adhesion energy, γ, dropped by more than one order of magnitude while the shear strength, τ, decreased to a lesser extent. Our observations indicate that, for a platinum-coated tip on mica, $\tau \propto \gamma^{0.44}$. This is a new observation of a relation between adhesion and friction and is not explained by existing theories.

Introduction

While the phenomena of adhesion, friction, and wear between interacting surfaces in relative motion have been studied for centuries,[2] experimental techniques to investigate such phenomena at the molecular and atomic level have only recently been developed. Most notably, the surface forces apparatus (SFA),[3−6] the quartz-crystal microbalance,[7−9] and the atomic force microscope (AFM)[10,11] have begun to establish an understanding of tribology at the nanometer scale.

We have constructed an ultrahigh vacuum AFM[12] to investigate atomic-scale tribological properties. In particular, we are interested in studying the wearless interfacial friction of a single asperity. The AFM is an ideal instrument for these studies because it can simultaneously measure both normal and lateral forces between a tip and a sample with atomic-scale contrast.[10] Microfabrication techniques can produce sharp and robust tips typically with radii < 100 nm. If externally applied loads are kept low, then the AFM tip forms a nanometer-sized single asperity contact with the sample being probed, and interaction forces can be measured without causing damage.

However, some difficulties occur when using AFM to study nanotribology. In general, the exact chemical nature of the interface is not known, since contamination may be present. To reduce the effect of contamination and attempt to control the surface chemistry, we operate our AFM under ultrahigh vacuum conditions. Another drawback of the AFM is that precise calibration of the forces is difficult. This is mainly because the cantilever force constants are usually unknown. We will address the issues of AFM force calibration in an upcoming paper.[13] For the work presented in this paper, the forces quoted are estimates based upon calculations as described below. However, most of the phenomena we will discuss are in fact independent of the force calibration.

The final problem is that the contact area between the tip and sample cannot be directly measured and is difficult to infer unless the exact tip shape is known. There is no way at present to directly measure the tip−sample contact area with a conventional AFM. However, the tip shape can be determined with some precision if a suitable sample is utilized.[14] We have previously shown that measurable differences in frictional behavior can be associated with different tip sizes and shapes.[15] This was determined by investigating the frictional properties of a platinum-coated AFM tip in contact with a mica sample cleaved in ultrahigh vacuum (UHV). Utilizing contact mechanics, the interfacial adhesion energy and shear strength of the contact can be determined. The theoretical framework involved in this analysis is described below, followed by experimental measurements of shear strength and interfacial adhesion energy for the platinum-coated tip contacting mica in UHV.

Theoretical Background

As reported previously,[15] we have observed that the frictional force on a platinum-coated AFM tip in contact with mica in UHV

† Also at Department of Physics, University of California at Berkeley.

‡ Permanent address: Instituto Universitario de Ciencia de Materiales, "Nicolás Cabrera" Laboratorio de Bajas Temperaturas, C-III, Universidad Autónoma de Madrid, 28049 Madrid, Spain.

* Author to whom correspondence should be sent. Phone: (510) 486-6704. Fax: (510) 486-4995. E-mail: salmeron@stm.lbl.gov.

⊗ Abstract published in *Advance ACS Abstracts,* June 1, 1996.

(1) Johnson, K. L.; Kendall, K.; Roberts, A. D. *Proc. R. Soc. London, Ser. A* **1971**, *324*, 301.

(2) Dowson, D. *History of Tribology*; Longman: London, 1979.

(3) Tabor, D.; Winterton, R. H. S. *Proc. R. Soc. London, Ser. A* **1969**, *312*, 435.

(4) Israelachvili, J. N.; McGuiggan, P. M.; Homola, A. M. *Proc. R. Soc. London, Ser. A* **1972**, *331*, 19.

(5) Israelachvili, J. N.; McGuiggan, P. M.; Homola, A. M. *Science* **1988**, *240*, 189.

(6) Israelachvili, J. N.; McGuiggan, P. M.; Gee, M. L. *Wear* **1990**, *136*, 65.

(7) Krim, J.; Watts, E. T.; Digel, J. *J. Vac. Sci. Technol., A* **1990**, *8*, 3417.

(8) Watts, E. T.; Krim, J.; Widom, A. *Phys. Rev. B* **1990**, *41*, 3466.

(9) Krim, J.; Solina, D. H.; Chiarello, R. *Phys. Rev. Lett.* **1991**, *66*, 181.

(10) Mate, C. M.; McClelland, G. M.; Erlandsson, R.; Chiang, S. *Phys. Rev. Lett.* **1987**, *59*, 1942.

(11) Binnig, G.; Quate, C. F.; Gerber, C. *Phys. Rev. Lett.* **1986**, *56*, 930.

(12) Dai, Q.; Vollmer, R.; Carpick, R. W.; Ogletree, D. F.; Salmeron, M. *Rev. Sci. Instrum.* **1995**, *66*, 5266.

(13) Carpick, R. W.; Ogletree, D. F.; Salmeron, M. *Rev. Sci. Instrum.*, submitted.

(14) Sheiko, S. S.; Möller, M.; Reuvekamp, E. M. C. M.; Zandbergen, H. W. *Phys. Rev. B* **1993**, *48*, 5675.

(15) Carpick, R. W.; Agraït, N.; Ogletree, D. F.; Salmeron, M. *J. Vac. Sci. Technol., B* **1996**, *14*, 1289.

S0743-7463(95)00900-0 CCC: $12.00

varies with externally applied load in proportion to the contact area predicted by the Johnson−Kendall−Roberts (JKR)[1] theory of adhesive elastic contacts. Below, we summarize the principles of the JKR theory. More detailed discussions are available elsewhere.[16,17]

The JKR theory is a continuum contact mechanical model that considers the effect of surface energy on the properties of an elastic contact. It can be viewed as an extension of Hertzian contact mechanics[18] to include the effect of adhesion. The initial formulation of the theory was applied to the case of two spheres (approximated as paraboloids) in contact, which is equivalent to a sphere−plane contact by considering one sphere to have an infinite radius of curvature. The validity of the JKR model has been verified by SFA experiments.[19] The model can also be extended to more general shapes.[15,20,21]

The interface is considered to possess an energy per unit area $\gamma = \gamma_1 + \gamma_2 - \gamma_{12}$, where γ_1 and γ_2 are the respective surface energies and γ_{12} is the interfacial energy. γ is equivalent to the Dupré energy of adhesion, which corresponds to the work per unit area required to separate the surfaces from contact to infinity. However, the JKR approximation assumes that all the interaction forces have zero range. As such, the parameter γ effectively encompasses all attractive interaction forces.

The JKR theory allows the determination of several mechanical properties of the contact, including the pressure distribution, the indentation depth, and the contact area. The contact area A as a function of externally applied load L is given by

$$A^{3/2} = \frac{\pi^{3/2}R}{K}[L + 3\pi R\gamma + \sqrt{6\pi R\gamma L + (3\pi R\gamma)^2}] \qquad (1)$$

where R is the tip radius and K is the reduced elastic modulus of the two materials, given by

$$K = \frac{4}{3}\left[\frac{1-\nu_1^2}{E_1} + \frac{1-\nu_2^2}{E_2}\right]^{-1} \qquad (2)$$

with E_1 and E_2 the respective Young's Moduli, and ν_1 and ν_2 the respective Poisson's ratios. The Hertz formula is recovered by setting $\gamma = 0$.

The theory predicts that a finite negative load is required to separate the surfaces. This value is often referred to as the critical load and is given by

$$L_c = -\frac{3}{2}\pi R\gamma \qquad (3)$$

This is equivalent to the pull-off force measured in AFM experiments (if the tip is truly parabolic). At the critical load, a finite contact area exists. We shall refer to this area as the critical area, A_c, which is given by

$$A_c = \pi\left[\frac{3\pi\gamma R^2}{2K}\right]^{2/3} \qquad (4)$$

Let us assume that the frictional force is proportional to the area of contact. SFA experiments with contacting mica surfaces having either contaminant or liquid layers in between them have shown that, in the absence of wear, the frictional force F_f is directly proportional to the contact area;[22] i.e.,

$$F_f = \tau A \qquad (5)$$

where τ is the shear strength. Note that this means there will be a finite frictional force at the pull-off point, which we shall call the critical friction, F_c, given by

$$F_c = \tau A_c = \pi\tau\left[\frac{3\pi\gamma R^2}{2K}\right]^{2/3} \qquad (6)$$

The JKR equation can then be rewritten in the following compact nondimensional form

$$\hat{F}_f = [1 + \sqrt{1 + \hat{L}}]^{4/3} \qquad (7)$$

where the load and friction have been parametrized in terms of the critical load and critical friction:

$$\hat{F}_f = \frac{F_f}{F_c} \quad \text{and} \quad \hat{L} = \frac{L}{|L_c|} \qquad (8)$$

The above discussion shows that although four physical quantities are involved in the friction−load equation (adhesion energy, tip radius, modulus, and shear strength), there are only two independent parameters in the equation: L_c (eq 3) and F_c (eq 6). These two quantities (or any other single pair of points (L, F) on the curve) determine the entire shape of the curve. Furthermore, if R and K are known, then the JKR theory gives the interfacial adhesion energy γ and the shear strength τ from the measured L_c and F_c.

Experimental Section

The mica sample is held fixed in a sample holder inside the UHV chamber; the exact arrangement is described elsewhere.[12] A thin steel foil is epoxied on top of the mica sample and protrudes outward far enough to be grabbed by a manipulator. Using the manipulator, the foil is pulled off and carries a few layers of mica with it, exposing a fresh mica surface. The AFM is then brought into range to perform the experiment.

All data were acquired with a single Si_3N_4 cantilever[23] which was coated with nominally 100 nm of platinum. Our experience has shown that metal-coated AFM tips may lose the coating at the end of the tip due to tip−sample contact. To avoid this, the platinum was deposited after a brief plasma etch of the lever and tip which promotes adherence. To determine if the platinum coating remained on the end of the tip, we placed the tip in contact with a conducting sample and measured a low-contact resistance (1.5 kΩ including lead resistance) both before and after acquiring all the data described below. The resistance did not vary appreciably with applied load, even just before pull off. Since Si_3N_4 is an insulator, we conclude that, throughout the experiment, the platinum coating was not removed. These resistance measurements were carried out at atmospheric pressure.

The chamber pressure during the friction experiments was 7 $\times 10^{-8}$ Pa or less, and all experiments were performed with the system at room temperature.

To acquire our data, we simultaneously measure the normal and lateral bending of the AFM cantilever as it is scanned laterally across the sample while the applied load is sequentially stepped.[24] Figure 1 shows a typical friction trace for a single line scan at a constant applied load. The tip initially sticks to the mica, but once some critical lateral force is reached, it quickly slips laterally by one atomic spacing, where it sticks again. As the scan continues, the lever twist increases until the critical lateral force is again achieved and slip takes place. Equivalent behavior results when the scan direction is reversed. This atomic-scale stick−slip behavior is commonly observed in friction force microscopy.[10] To eliminate any offset in the lateral force signal, we calculate half the difference between the critical lateral force signals measured for the two scanning directions, as indicated in Figure 1. Each line scan is acquired at a fixed applied load; then the load is changed slightly, and another line scan is recorded. Two hundred and fifty-six line scans are recorded for each run. Each run is acquired in roughly 30 s. A typical plot for a single run is shown in Figure 2. Other than the averaging, the data are unprocessed.

(16) Israelachvili, J. N. *Intermolecular and Surface Forces*, 2nd ed.; Academic Press, Inc.: San Diego, CA, 1992.
(17) Johnson, K. L. *Contact Mechanics*; University Press: Cambridge, 1987.
(18) Hertz, H. *J. Reine Angew. Math.* **1881**, *92*, 156.
(19) Israelachvili, J. N. In *Fundamentals of Friction*; Singer, I. L., Pollock, H. M., Ed.; Kluwer: Dordrecht, 1992; p 351.
(20) Maugis, D.; Barquins, M. *J. Phy. D: Appl. Phys.* **1983**, *16*, 1843.
(21) Maugis, D. *Langmuir* **1995**, *11*, 679.
(22) Homola, A. M.; Israelachvili, J. N.; Gee, M. L.; McGuiggan, P. M. *J. Tribol.* **1989**, *111*, 675.
(23) Nanoprobe, Digital Instruments, Santa Barbara, CA.
(24) Hu, J.; Xiao, X.-D.; Ogletree, D. F.; Salmeron, M. *Surf. Sci.* **1995**, *327*, 358.

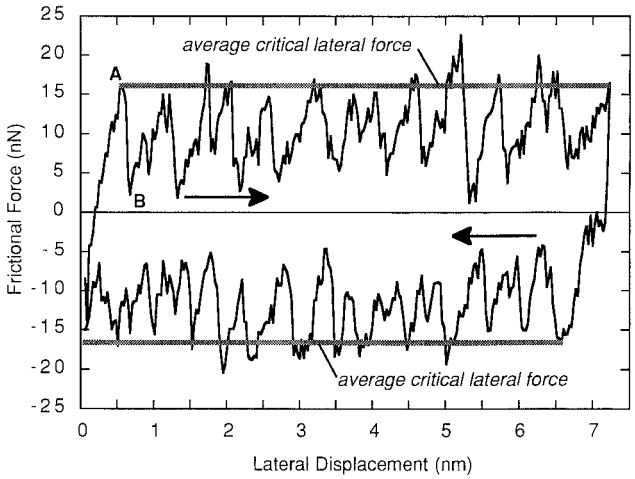

Figure 1. Bidirectional friction signal trace at a constant applied load. The tip initially sticks to the surface until some critical lateral force is achieved (point A). At this point, the tip slips laterally and sticks again (point B), where the kinetic energy of the lever and tip is lost to the contacting bodies. This behavior essentially repeats once every atomic spacing until the scan direction is reversed, whereupon the equivalent inverse behavior occurs. The arrows indicate the scan direction. The lateral force where slip occurs is seen to be nearly constant.

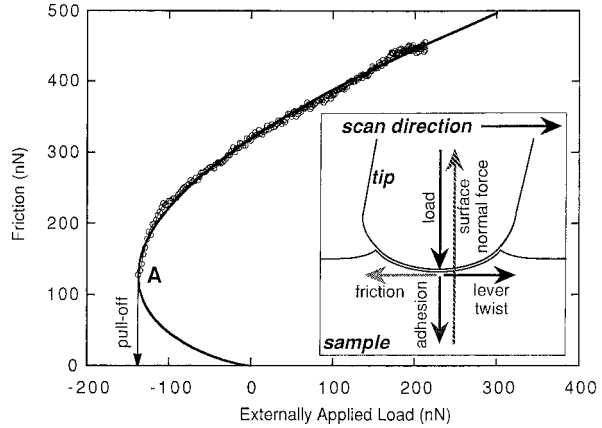

Figure 2. Characteristic friction vs load plot for a platinum-coated tip on mica cleaved in UHV (open circles) from a single run. The *x*-axis corresponds to externally applied load, i.e. normal cantilever displacement. The zero point is given by the normal cantilever displacement out of contact with the sample. The friction axis corresponds to the average critical lateral force measured for each value of the applied load, as described in Figure 1. Note the nonlinear dependence of friction with load and the finite frictional force at the pull-off point (A). The solid line is the JKR curve for contact area vs load. The curve is fit to the critical load and to the value of the friction at zero applied load to match the acquired data. The lower branch of the JKR curve is mechanically unstable: the surfaces are predicted to spontaneously separate at point A. The inset is a diagram of the net forces acting on the tip (tip size, contact area, and indentation are not drawn to scale): while scanning, the twisted lever (not shown) wants to push the tip forward but friction resists this motion (the tilt angle of the tip is greatly exaggerated). The external load applied by the lever along with the tip−sample adhesion force are balanced by the resultant surface normal force. Of course, pressure is distributed throughout the contact area.

These measurements can be performed over any desired load range that is attainable with the particular lever used. For these experiments, we usually begin the measurements at a substantial positive load which is decreased until the tip pulls out of contact with the sample. No significant difference is observed if the data are acquired while increasing the load except that, due to the jump-to-contact instability, the low-load portion of the friction vs load curve is not accessed.

At very high loads with mica in UHV, anomalously large lateral forces result indicating the onset of wear of the surface, similar to effects seen in air.[24] For these experiments, all friction data were acquired with the externally applied load remaining well below the wear threshold. Such wear events permanently damage the mica surface and can be imaged in the topographic mode after they occur. Regular imaging of the mica surface confirmed that repeated scanning on the same part of the sample did not instigate wear although in most cases data were acquired over a new area of the mica surface.

Lever spring constants were calculated from formulae derived using continuum elasticity theory.[25] Our formulae are similar to those recently described by Sader,[26] which compare favorably to sophisticated finite element analysis of lever mechanical properties.[27] To estimate the spring constants, we measured the dimensions of the levers with a scanning electron microscope and used the best available estimates of material properties. As such, we expect our force estimates to be good within at least a factor of two. A detailed discussion of force calibration with an AFM will be presented in a separate publication.[13]

Results and Discussion

Friction and JKR Theory. Figure 2 shows a typical friction vs load plot for the platinum-coated tip on mica in UHV. The *x*-axis corresponds to the externally applied load, i.e. normal cantilever displacement. The zero point is given by the cantilever position out of contact with the sample when no normal force is acting. The friction is nonlinear with load, especially near the pull-off point. Clearly, there is a finite frictional force at the pull-off point. The critical load observed while scanning laterally scaled with the pull-off force measured from force−distance curves that are acquired without lateral scanning but was usually of smaller magnitude. These "premature" pull-off events may be due to increased instabilities during scanning or may be a consequence of the influence of the lateral force on the interface.[28] This effect will be discussed in more detail elsewhere.[29]

Figure 2 also shows the JKR curve overlaid for comparison. Clearly, the agreement is very good. As mentioned above, the JKR solution applies for a parabolic tip. Different tip shapes will produce a different functional dependence of friction upon load. In other words, one can distinguish between the friction−load relation for a parabolic tip and, for example, a flatter tip profile.[15] We therefore acquired a cross-sectional profile of the tip before this set of data was acquired. This was done by imaging the faceted $SrTiO_3$(305) surface discussed by Sheiko et al.[14] This sample consists of a large number of facets which form long, sharp unidirectional ridges. The apex of each ridge is typically much sharper than the AFM tip, and so a topographic scan over a ridge produces an "image" of the AFM tip. One such profile is displayed in Figure 3. The tip is essentially parabolic with an effective radius of ∼140 nm. A profile orthogonal to this one was obtained by rotating the crystal by 90° and yielded the same result. This information about the tip shape is thus consistent with the observed friction−load relation.

We were further convinced of the applicability of the JKR model by deliberately blunting the tip with large loads, after the data presented here were acquired. The frictional behavior of the modified tip correlated with that predicted for a flatter tip profile, determined by extending

(25) Timoshenko, S. P.; Goodier, J. N. *Theory of Elasticity*; McGraw Hill: New York, 1987.
(26) Sader, J. E. *Rev. Sci. Instrum.* **1995**, *66*, 4583.
(27) Sader, J. E.; Larson, I.; Mulvaney, P.; White, L. R. *Rev. Sci. Instrum.* **1995**, *66*, 3789.
(28) Savkoor, A. R. In *Fundamentals of Friction*; Singer, I. L., Pollock, H. M., Ed.; Kluwer: Dordrecht, 1992; p 111.
(29) Carpick, R. W.; Agraït, N.; Ogletree, D. F.; Salmeron, M. In progress.

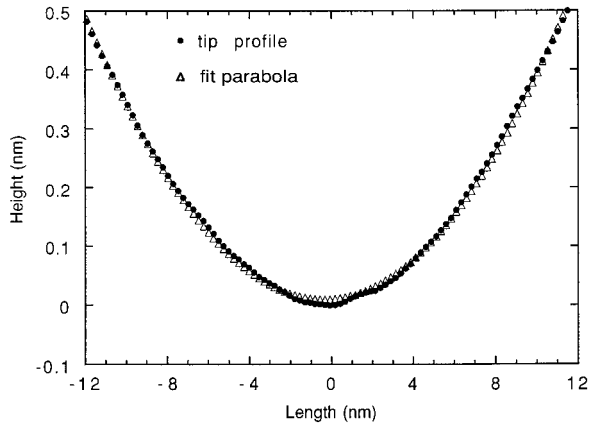

Figure 3. Tip profile acquired by scanning the $SrTiO_3(305)$ sample in air, taken before the tip was placed in vacuum and the data in Figure 1 were acquired. The actual tip profile is plotted with solid circles, and a parabolic fit is plotted with open triangles for comparison. The tip profile is essentially parabolic, with an effective tip radius of ~140 nm.

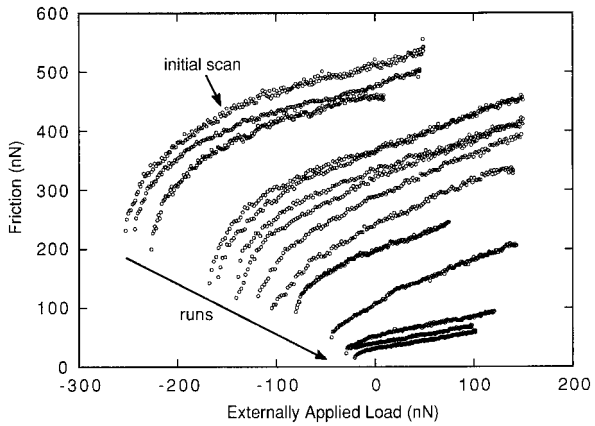

Figure 4. Selection of friction−load plots from several runs. Not every run is shown, as the data would be too closely spaced to distinguish separate plots. The pull-off force, L_c, decreased monotonically by about 0−5% from one run to the next. The frictional force at pull off, F_c, also decreased monotonically from one run to the next. This corresponds to monotonic decreases in the interfacial energy and the shear strength.

the JKR model for different tip shapes. A subsequent profile of the $SrTiO_3(305)$ sample showed that indeed the tip had been flattened. The details of these results are discussed elsewhere.[15] We have also performed experiments with cantilevers fabricated from Si_3N_4 and doped Si. In these experiments, the frictional force was also proportional to the JKR solution for contact area. The results with Si and Si_3N_4 tips will be discussed elsewhere.[29]

The JKR theory is not the only description of bodies in adhesive contact but is rather the limiting case of a continuous regime of contact mechanics. The JKR regime is most appropriate when softer materials with strong short-range adhesion are in elastic contact. Contact between stiff materials with long-range attraction are better described by the Derjaguin−Müller−Toporov (DMT)[30] theory. We have attempted to fit our data by a DMT-like fit, but the quality was much poorer. This is mainly because the DMT theory predicts zero contact area at the pull-off point; in contrast we always observe a finite frictional force at the pull-off point. Even adding a finite offset to the frictional forces fails to make the DMT fit better than the JKR fit.

The transition between these two limits is discussed by Johnson,[31] as well as by Maugis,[32] and Müller et al.[33] Summarizing briefly, the following dimensionless parameter determines which limit is appropriate:

$$\mu = \left[\frac{16R\gamma^2}{9K^2 z_0^3}\right]^{1/3} \tag{9}$$

where z_0 represents the equilibrium separation of the surfaces, i.e. the effective range of adhesion. To be firmly in the JKR limit, μ should be about 5 or greater, whereas $\mu < 0.1$ implies the DMT limit. Values in between correspond to a "transition region" where the area−load relation is complicated to evaluate. Unfortunately, we cannot unambiguously determine μ since (i) our calibration is uncertain, leading to a possible error in the value of γ, and (ii) the exact value of z_0 is unknown and thus somewhat arbitrary although we expect short-range adhesion forces to dominate in vacuum. For our data, using $z_0 = 0.2$ nm, estimates for μ fall within the transition region, from about 0.2 to 1.1. Our apparent agreement with the JKR fit could be explained if we have underestimated the normal forces; thus, the adhesion energy is actually larger than our measurements. We plan to carefully examine these questions once we can calibrate the AFM cantilevers more accurately.

Whichever contact mechanical description is most appropriate, it is important and surprising that a continuum model can account very accurately for the behavior of a nanometer-sized contact which exhibits lateral atomic-scale stick−slip behavior. This is plausible at high loads, where for each load step (typically 1 nN or less) the corresponding change in contact area, using the continuum model, would only be a few mica unit cells. Elastic relaxations of tip and sample atoms can easily smooth out the changes in contact area. However, the rate of change of area with load increases as the load decreases (cf. Figure 2) and in fact diverges at the pull-off point. We might therefore expect to see, at low loads, a transition from a smooth friction−load curve to one that has steps as significant numbers of unit cells make or break contact in an "avalanching" fashion.[34,35] For the tip used in this experiment, we did not observe such behavior. However, very recently, we observed distinct steps in the frictional force at low loads in an experiment with a similar platinum-coated AFM tip on mica in UHV. This behavior was not fully reproducible and must be investigated further before we can conclude that we are seeing a continuum-atomistic transition.

Changes in Friction and Adhesion. Another surprising finding of this study was the variation of the frictional properties of the platinum tip on mica as a result of repeated scanning. For the initial set of data (before the tip was blunted), every friction curve obtained could be fit with a JKR curve. However, the values of L_c and F_c changed with repeated scanning. In particular, both L_c and F_c were seen to decrease slightly from one run to the next (less than 5% per run). Figure 4 displays a selection of the friction−load curves obtained. Clearly, L_c and F_c progressively decrease as runs are performed, which after many runs results in a large overall change. Each run was performed over a new area of the mica surface.

(30) Derjaguin, B. V.; Muller, V. M.; Toporov, Y. P. *J. Colloid Interface Sci.* **1975**, *53*, 314.
(31) Johnson, K. L. *Langmuir,* in press.
(32) Maugis, D. *J. Colloid Interface Sci.* **1992**, *150*, 243.
(33) Müller, V. M.; Yushenko, V. S.; Derjaguin, B. V. *J. Colloid Interface Sci.* **1980**, *77*, 91.
(34) Pollock, H. M. In *Fundamentals of Friction*; Singer, I. L., Pollock, H. M., Ed.; Kluwer: Dordrecht, 1992; p 77.
(35) Pethica, J. B.; Sutton, A. P. *J. Vac. Sci. Technol., A* **1988**, *6*, 2494.

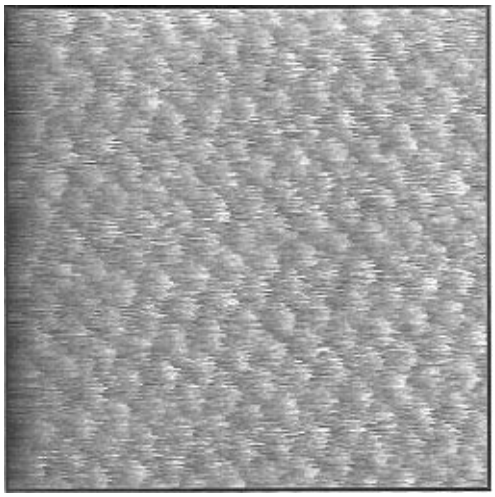

Figure 5. Atomic lattice resolution lateral force image of the mica sample (6.4×6.4 nm^2) taken in between a set of friction−load measurements. The contrast is due to stick−slip motion which has an amplitude of 10 nN. We were able to acquire such images routinely throughout the entire set of measurements.

Throughout the experiment, we were able to obtain atomic lattice resolution images of the mica surface (Figure 5). Despite the dramatic change in frictional forces that occurred, no noticeable changes were observed in the atomic-lattice resolution images. This does not rule out any changes of the tip but merely indicates that the stick−slip behavior persisted.

Table 1 shows the largest and smallest values of L_c and F_c that we measured for the initial set of experiments, as well as for the blunted tip. Using the JKR theory, we also calculated the corresponding interfacial adhesion energy, shear strength, and contact area at pull off. We have also indicated, for the initial tip, the elastic indentation depth and the mean pressure for a positive externally applied load equal to the magnitude of the critical load. To perform these calculations, we used a Young's modulus of 56.5 GPa and a Poisson's ratio of 0.098 for the mica *c*-axis calculated from recent Brillouin scattering data,[36] and a Young's modulus of 177 GPa and a Poisson's ratio of 0.39 for platinum.[37] These calculations are based upon estimates of the lever force constants, as mentioned above. However, errors due to calibration should be systematic. Table 1 is mostly intended to provide a sense of the order of magnitude of these quantities, along with the relative change of these quantities between the high and low adhesion conditions.

The uncertainty due to calibration does not affect the functional dependence of shear strength upon adhesion. For each set of data in Figure 4, F_c and L_c can be determined. Figure 6 shows a plot of F_c vs L_c. The dependence is nearly linear. Since L_c is proportional to γ (eq 3), while F_c is proportional to $\tau\gamma^{2/3}$ (eq 6), this implies that τ is only weakly dependent upon γ. This assumes R is constant (see below). By calculating τ and γ for each point (F_c, L_c) in Figure 6, we determined that $\tau \propto \gamma^{\nu}$, where $\nu \cong 0.44 \pm 0.10$.

Only a change in the surface of the tip, either structural or chemical, can explain our observations. We established that this adhesion decrease was related to the tip, and was induced by scanning the tip in contact with the mica as follows. The change in L_c and F_c did not depend upon the time interval between runs, as one might expect if there was some sort of accumulating surface contamination. For example, some of the curves in Figure 4 were in fact acquired 12−24 h apart, whereas most of the other curves were acquired a few minutes apart, yet the changes in L_c and F_c are about the same from one curve to the next. Our microscope is capable of coarse lateral position adjustment, and so we took advantage of this by positioning the cantilever over several new regions of the sample. The subsequent values of L_c and F_c continued to monotonically decrease, independent of the imaging location. We also investigated whether or not a brief tip−sample contact had any effect. This was done by taking several force−distance curves. Without scanning, the tip−sample separation was varied, bringing the tip in and out of contact with the sample. The force required to pull the tip out of contact with the sample corresponds to L_c. We were not able to cause L_c to decrease simply by acquiring force-distance curves. Finally, we rule out any change in the large-scale structure of the tip to account for the adhesion decrease. As mentioned above, changes in the tip shape are clearly reflected in the friction−load curve. Our friction−load curves were all consistent with a parabolic tip profile and inconsistent with any substantially different tip profile. Furthermore, looking at eqs 3 and 6, for L_c and F_c to decrease would require the tip radius R to systematically shrink! In summary, L_c and F_c decreased *if and only if the tip was scanned in contact* with the sample. Since a JKR curve can describe each friction spectrum and R and K were constant, we conclude that the variation of L_c and F_c corresponds to changes in the interfacial adhesion energy γ and the shear strength τ brought about by changes in the *interfacial* chemistry or structure induced by scanning.[38]

Since we are unable to spectroscopically analyze the tip−sample interface, any explanations at this point are purely conjectural. One possible chemical change worth discussing is scanning-induced transfer of potassium from the mica surface to the tip. Potassium adsorption is not unreasonable considering the following plausibility argument. The mica cleavage plane exposes potassium ions which are strongly bound to the mica surface, but during tip−sample contact there is a finite probability that a potassium atom will transfer to the metal tip and adsorb. An energetic barrier to this process as well as diffusion of potassium on the platinum tip[39] would necessitate repeated transfer events to eventually saturate the end of the tip. This is consistent with the observation of a gradual, scan-by-scan change in adhesion. Potassium adsorption lowers the surface free energy of the platinum; thus, the work of adhesion will decrease as potassium adsorbs, since the sample, being much larger than the contact zone itself, provides an infinite reservoir of potassium to replenish vacancies in the mica surface. In other words, the partially potassium-covered tip will not have as strong a chemical attraction to the potassium-covered mica surface as a cleaner metal tip would. Note that our estimated total decrease in the work of adhesion is ~0.39 J/m^2 (see Table 1). The energy of adsorption of potassium on the clean Pt(111) surface at one monolayer coverage in UHV has been measured to be ~0.94 J/m^2,[39] which is of the same order of magnitude. Attributing the adhesion energy decrease to potassium adsorption is therefore not physically unreasonable.

(36) McNeil, L. E.; Grimsditch, M. *J. Phys.: Condens. Matter* **1992**, *5*, 1681.

(37) *Metals Handbook*, 10th ed.; American Society for Metals: Metals Park, OH, 1990.

(38) Since the decrease of γ and τ occurs during scanning, fitting each of the friction−load curves to the JKR equation is not strictly correct, since fixed values of γ and τ are assumed for such a fit. However, the changes in these values were sufficiently small so that ignoring them for an individual fit introduces a negligible error. In fact, adapting the JKR equation to take such changes into account has a negligible effect (Johnson, K. L. Personal communication).

(39) Garfunkel, E. L.; Somorjai, G. A. *Surf. Sci.* **1982**, *115*, 441.

Table 1

	critical load L_c (nN)	critical friction F_c (nN)	interfacial adhesion energy γ (J/m^2)	shear strength τ (GPa)	contact area at pull off (nm^2)	elastic depth at $L = +\|L_c\|$ (nm)	mean pressure at $L = +\|L_c\|$ (GPa)
max.	267	210	0.404	0.91	230	0.75	0.36
min.	12	7.9	0.019	0.27	29	0.10	0.13
blunted	134	262	0.102	0.71	370		

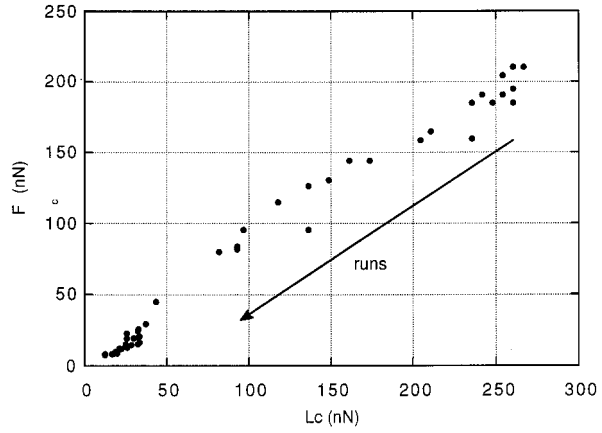

Figure 6. Plot of the values of F_c and L_c measured from a large number of runs, some of which are displayed in Figure 4. The dependence is nearly linear. The interfacial energy γ and the shear strength τ were calculated for each point. Fitting this to a power law $\tau \propto \gamma^{\nu}$ gives $\nu \cong 0.44 \pm 0.10$.

Another possibility is a structural rearrangement of tip atoms at the interface caused by sliding. It has been postulated that changes in the atomic commensurability of contacting surfaces would cause changes in friction and adhesion.[40−42] Increased commensurability is expected to increase friction and possibly adhesion, as tip and sample atoms can "lock together" more easily. Indeed, mica surfaces in contact that were rotated with respect to one another produced maximum adhesion[41] and friction[42] when the orientation of the two mica sheets matched.[43] From this point of view, the observed decrease in friction and adhesion with scanning implies that scanning reduces commensurability. Whether this occurs in our case is not known, and it is not obvious that the tip structure should have any degree of commensurability with the mica to begin with. Nevertheless, further experiments are needed to investigate this interesting possibility.

In any case, it is remarkable that such a dramatic change in friction and adhesion occurs as a result of interfacial changes. Order of magnitude changes in adhesion and friction can thus occur even though bulk properties such as the phonon spectrum and specifically the elasticity, which also play crucial roles in determining friction, are unchanged. Interestingly, we did not observe such a variation of adhesion and friction in experiments with either silicon or silicon nitride tips on mica in UHV; the adhesion energy and shear strength remained essentially constant during all runs. This may reinforce the idea that the chemistry of the surface of the tip plays a role, as platinum has very different chemistry than the expected passive terminations of silicon or silicon nitride tips. Alternately, platinum is more ductile than silicon and silicon nitride, which are fairly brittle materials. Thus, a structural change in the tip termination brought about by shear forces is also more likely to occur with platinum.

As mentioned above, the platinum-coated tip was blunted after this set of experiments and further friction measurements were performed. This was followed by measuring the contact resistance between the tip and a conducting sample, which confirmed that the platinum coating had not been removed. Immediately after blunting the tip, the adhesion and friction recovered but again progressively decreased with scanning. We also determined the new, blunted tip shape using the $SrTiO_3$ sample afterward. From these measurements, we estimate that, immediately after blunting the tip, the interfacial adhesion energy had recovered to a value in between the initial and final values measured before blunting the tip. This further supports the idea that the tip chemistry is affecting the adhesion, since blunting the tip presumably exposes new unreacted platinum, thus restoring the adhesion.

The weak dependence of the shear strength upon the adhesion is a surprising result. In the most simple case, one might expect τ to be linearly proportional to γ. A simple model relating surface energy and shear strength in the absence of wear is the so-called "Cobblestone Model".[22,44−46] Surfaces sliding with respect to one another are considered in a similar fashion to the wheels of a cart rolling over a cobblestone street. If at rest, the wheels will be settled into grooves between the cobblestones. To initiate motion, a lateral force is required to lift the wheels out of the grooves and over the cobblestones. In this model, the force of gravity is replacing the attractive surface forces. For an atomically smooth sample, the "cobblestones" could represent the atomic corrugation. SFA experiments for contacts between hydrocarbon surfaces or surfaces with layers of liquid molecules in between show general agreement with the model.[19,22,46] However, the model predicts that the shear strength is linearly proportional to the interfacial surface energy ($\nu = 1$),[19] which we do not observe in this case.

Another model relating friction and adhesion has been proposed by Israelachvili.[19,47] Experiments with the SFA have shown that, for systems of chainlike molecules between contacting surfaces, the adhesion energy increases while surfaces are in contact. Hysteresis of the contact area then occurs between approach and retraction of the surfaces, and evidence suggests that frictional forces are larger when adhesion hysteresis is larger. However, this is inconsistent with our observations, as we do not observe any frictional hysteresis when comparing increasing and decreasing loading. Israelachvili's theory is based on studies of particular molecular structures such as long hydrocarbon chain molecules, whereas according to the theory adhesion hysteresis is not expected for solid−solid contacts. The theory attributes the hysteresis to complex phenomena occurring at the interface, namely reorientation, interdiffusion, and interdigitation of the

(40) Sokoloff, J. B. *Wear* **1993**, *167*, 59.
(41) McGuiggan, P. M.; Israelachvili, J. N. *J. Mater. Res.* **1990**, *5*, 2232.
(42) Hirano, M.; Shinjo, K.; Kaneko, R.; Murata, Y. *Phys. Rev. Lett.* **1991**, *67*, 2642.
(43) However, the presence of adhesion and friction anisotropy depended upon the experimental environment. Adhesion anisotropy occurred in humid air (33% RH) but not in dry nitrogen. Friction anisotropy occurred in dry air at higher temperature (130 °C) but not in ambient air.
(44) Sutcliffe, M. J.; Taylor, S. R.; Cameron, A. *Wear* **1978**, *51*, 181.
(45) McLelland, G. M. *Adhesion and Friction;* Springer Series in Surface Science; Springer: New York, 1989; Vol. 17.
(46) Homola, A. M.; Israelachvili, J. N.; McGuiggan, P. M.; Gee, M. L. *Wear* **1990**, *136*, 65.
(47) Yoshizawa, H.; Chen, Y.-L.; Israelachvili, J. *Wear* **1993**, *168*, 161.

molecules. These processes have long relaxation times which are comparable to the time the surfaces spend in contact with each other, and so equilibrium is not reached during contact. In contrast, we do not expect processes with long relaxation times to occur on surfaces in UHV, as the interface is much less complex. Also, the model predicts a cyclical hysteresis as opposed to the progressive changes in adhesion and shear strength which we observe.

It is thus not clear yet whether the observed power law represents a very specific case of the friction−adhesion relation for the particular platinum−mica system studied here or is a more general phenomenon. More experiments with other systems are needed to understand this important relation.

Summary

The frictional properties of a platinum-coated AFM tip in elastic contact with mica in UHV are accurately described by the JKR theory of contact mechanics, assuming that the frictional force is proportional to the area of contact. We observe a surprising scanning-induced reduction of the tip−sample adhesion and friction that we believe is due to changes in the chemical or structural composition of the surface of the AFM tip. The shear strength was affected much less than the adhesion energy, a result which calls for a more detailed theoretical analysis. Clearly, experiments where the interfacial composition is more controlled or determinable are needed. We plan to address this with future experiments in UHV.

Acknowledgment. We gratefully acknowledge Prof. K. L. Johnson for very useful discussions. We would like to thank A. Lyon for coating the AFM levers with platinum. RWC acknowledges the support of the Natural Sciences and Engineering Research Council of Canada. NA acknowledges the support of the Ministry of Education and Science of Spain. This work was supported by the Director, Office of Energy Research, Basic Energy Sciences, Materials Division of the US Department of Energy under Contract Number DE-AC03-76SF00098.

LA9509007